# research papers

# Synthesis and fading of eighteenth-century Prussian blue pigments: a combined study by spectroscopic and diffractive techniques using laboratory and synchrotron radiation sources

Louise Samain,[a]*‡ Fernande Grandjean,[b,c] Gary J. Long,[c] Pauline Martinetto,[d] Pierre Bordet,[d] Jana Sanyova[e] and David Strivay[a]

[a]Centre Européen d'Archéométrie, University of Liège, Sart Tilman B15, Liège 4000, Belgium, [b]Faculty of Sciences, University of Liège, Sart Tilman B5, Liège 4000, Belgium, [c]Department of Chemistry, Missouri University of Science and Technology, University of Missouri, Rolla, MO 65409-0010, USA, [d]Institut Néel, CNRS et Université Joseph-Fourier, BP 166, 38042 Grenoble, France, and [e]Institut Royal du Patrimoine Artistique, Parc du Cinquantenaire 1, Brussels 1000, Belgium. E-mail: louise.samain@ulg.ac.be

Prussian blue, a hydrated iron(III) hexacyanoferrate(II) complex, is a synthetic pigment discovered in Berlin in 1704. Because of both its highly intense color and its low cost, Prussian blue was widely used as a pigment in paintings until the 1970s. The early preparative methods were rapidly recognized as a contributory factor in the fading of the pigment, a fading already known by the mid-eighteenth century. Herein two typical eighteenth-century empirical recipes have been reproduced and the resulting pigment analyzed to better understand the reasons for this fading. X-ray absorption and Mössbauer spectroscopy indicated that the early syntheses lead to Prussian blue together with variable amounts of an undesirable iron(III) product. Pair distribution functional analysis confirmed the presence of nanocrystalline ferrihydrite, $Fe_{10}O_{14}(OH)_2$, and also identified the presence of alumina hydrate, $Al_{10}O_{14}(OH)_2$, with a particle size of $\sim 15$ Å. Paint layers prepared from these pigments subjected to accelerated light exposure showed a tendency to turn green, a tendency that was often reported in eighteenth- and nineteenth-century books. The presence of particles of hydrous iron(III) oxides was also observed in a genuine eighteenth-century Prussian blue sample obtained from a polychrome sculpture.

**Keywords: iron(III) hexacyanoferrate(II); archaeometry; pair distribution function; light exposure fading; paint layers.**

## 1. Introduction

The restoration of cultural heritage objects requires a good understanding of the various long-term degradation processes of the materials used in paintings and related artistic efforts. The interactions between pigments, binders and supports need to be investigated in order to understand any possible alterations with time. In this context Prussian blue is a particularly interesting artistic pigment because of its popularity among artists and its variable light fastness, a fastness that had already been questioned by the mid-eighteenth century.

Prussian blue was accidentally discovered in Berlin in 1704. It is now known to contain a hydrated iron(III) hexacyanoferrate(II) anion, $\{Fe^{III}[Fe^{II}(CN)_6].xH_2O\}^-$, with varying values of $x$ up to 16, and with various cations, such as $K^+$, $NH_4^+$

or $Na^+$. Its intense blue color arises from an intervalence electron transfer between the iron(II) and iron(III) ions when light is absorbed at $\sim 700$ nm.

Because of its low cost and its extremely high tinting strength, Prussian blue was widely used by artists from $\sim 1720$ until 1970 (Berrie, 1997). However, reports of the discoloration or fading of Prussian blue pigments had already been noted in eighteenth-century and nineteenth-century books (Mérimée, 1830; Riffault, 1850; Regnier, 1855). Even though the preparative methods of the Prussian blue pigments were rapidly recognized as a contributory factor in their fading (Kirby, 1993), to date, little attention has been devoted to obtaining a scientific understanding of the intrinsic degradation processes associated with Prussian blue pigments in paint layers (Kirby & Saunders, 2004; Samain et al., 2011, 2013).

Only two reagents are essential in the production of Prussian blue pigments by precipitation, an iron salt and an alkali

hexacyanoferrate. However, the chemical stoichiometry and structure of the starting materials and the resulting Prussian blue pigments were unknown in the eighteenth century. At that time potassium hexacyanoferrate was indirectly obtained from the calcination of animal matter with an alkali. The residue of this calcination was boiled in water yielding, after filtration, a pale yellow solution that presumably contained potassium hexacyanoferrate. This solution was then mixed with a solution of an iron(II) salt and alum, leading to the formation of a pale greenish precipitate that was filtered and, finally, treated with hydrochloric acid to yield Prussian blue.

In the mid-nineteenth century it became possible to produce potassium hexacyanoferrate in bulk from gas purification products (Krafft, 1854). Consequently, Prussian blue pigments could be manufactured by a completely inorganic process; these preparative methods are usually referred to as modern methods in order to distinguish them from the eighteenth-century methods that used an organic starting material. The modern inorganic manufacturing methods were rapidly standardized and industrialized, a process that rapidly led to the production of inexpensive high-quality Prussian blue pigments (Buxbaum & Pfaff, 2005).

The composition and quality of Prussian blue pigments synthesized according to the early eighteenth-century methods were much more variable because of the rather empirical character of the process. Ingredients and their proportions used in the eighteenth-century recipes have been studied and indexed in detail by Kirby & Saunders (2004) and Asai (2005). However, neither the underlying chemical reactions nor the interactive factors that influenced the light fastness of the pigments made in the eighteenth-century have been identified.

Herein, Prussian blue pigments have been synthesized according to two eighteenth-century recipes. The resulting powders have been characterized by high-energy X-ray powder diffraction and two iron-specific techniques, iron-57 transmission Mössbauer spectroscopy and iron $K$-edge X-ray absorption spectroscopy. In order to evaluate the light fastness of the synthesized pigments, the pure pigment powders were painted from arabic gum on watercolor paper and subjected to an accelerated light exposure for a period of up to 400 h. The paint layers were then studied by UV–visible spectroscopy. The results of these studies were then applied to the analysis of Prussian-blue-containing paint layers of an eighteenth-century polychrome sculpture.

## 2. Experimental

### 2.1. Sample preparation

Two syntheses that were reported in the eighteenth-century literature have been reproduced for this work. The first is based on the recipe developed by R. Dossie (Dossie, 1758) in 1758 and the second on the preparation described by M. Le Pileur d'Apligny (Le Pileur d'Apligny, 1779) in 1779. The original text of both recipes can be found in the electronic

**Table 1**
Reagent proportions for the two eighteenth-century recipes.

| Synthesis | Reagents proportion in parts | | | | |
| --- | --- | --- | --- | --- | --- |
| | Dried blood | Alkali, $K_2CO_3$ | Iron salt, $FeSO_4.7H_2O$ | Alum, $KAl(SO_4)_2$ $.12H_2O$ | Acid, HCl |
| Dossie | 3 | 1 | 1 | 2 | 4 or 0 |
| Le Pileur d'Apligny | 8 | 8 | 3 | 4 | 4 or 0 |

supplementary material.[1] The major difference between the two methods is the proportion of the ingredients used (see Table 1).

In the above syntheses, dried blood that is sold and used as a garden fertilizer by DCM Corporation, Grobbendonk, Belgium, was used as the organic matter. All other reagents used herein for the syntheses of eighteenth-century Prussian blue pigments were of reagent-grade quality and obtained from Sigma-Aldrich, Steinheim, Germany.

Appropriate amounts of dried blood and potassium carbonate, $K_2CO_3$, were mixed in a porcelain crucible and heated in a Nabertherm furnace; the temperature was increased from room temperature to 923 K in two hours. The mixture initially burned with an orange flame. At 723 K, after ∼90 min heating, the crucible was removed from the furnace and its contents mixed. Upon further heating to 923 K, no further combustion was observed and the contents of the crucible were reddish. The crucible was then removed from the furnace and the contents were dropped into ∼300 ml of boiling deionized water and the mixture was subsequently boiled for 45 min. After filtration, the pale yellow filtrate was collected and mixed with an aqueous solution of iron sulfate, $FeSO_4.7H_2O$, and alum, $KAl(SO_4)_2.12H_2O$, previously dissolved in deionized water. A pale-greenish precipitate immediately formed and was collected by filtration. A prolonged delay of several hours between the formation and the filtration of the greenish precipitate leads to the formation of an orange compound at the surface of the sediment.

Because two shades of Prussian blue were reported in the eighteenth century, a pale one and a dark one, the collected precipitate was divided into two fractions. The first part was treated with hydrochloric acid, in order to eliminate the aluminium compound present, and then thoroughly washed with deionized water. The product was finally air-dried and ground into a dark blue powder. The second part was only washed with deionized water so that the aluminium compound remained in the pigment as an extender. After air-drying and grinding, a pale green-blue powder was obtained.

Both syntheses were reproduced several times, first to determine the missing parameters in the recipes, such as the maximum calcination temperature and the duration of the calcination, and second to evaluate the reproducibility of the syntheses. A calcination temperature of at least 873 K was necessary to obtain a complete combustion of the dried blood.

---

[1] Supplementary data for this paper are available from the IUCr electronic archives (Reference: FV5008). Services for accessing these data are described at the back of the journal.

**Table 2**
Description and labels of the eighteen-century Prussian blues.

| Synthesis | | Labels | Color appreciation |
|---|---|---|---|
| Dossie | Immediate filtration, acid treatment | D1 | Dark blue |
| | No acid treatment, | D2 | Light blue–green |
| | + alumina hydrate | D3 | Light blue |
| Le Pileur d'Apligny | Immediate filtration, acid treatment | LPA1 | Intense dark blue |
| | Delayed filtration, acid treatment | LPA2 | Gray–blue |
| | No acid treatment, + alumina hydrate | LPA3 | Brown |

The duration of the calcination seems to be less critical but must be long enough to combust all of the animal matter between room temperature and 873 K. The liquor that is collected after filtration of the aqueous solution containing the residue of the calcination presumably contains potassium ferrocyanide. The yield of the synthesis is extremely small; although 30 g of dried blood was used in the Dossie synthesis, less than 1 g of Prussian blue was obtained. The same occurs for the Le Pileur d'Apligny recipe. The limiting reagent is most likely the hexacyanoferrate(II) complex, presumably formed by calcination of blood and potassium carbonate.

Although the synthesis is expected to be better controlled due to modern laboratory conditions in comparison with the situation in the eighteenth century, the reproducibility of the eighteenth-century recipes is problematic and the reproducibility attempts were not always successful. The critical step appears to be the filtration of the greenish precipitate followed by its washing with water. Before treatment with hydrochloric acid the precipitate should be light blue, presumably containing Prussian blue and aluminium hydroxide, now shown herein to be alumina hydrate, $Al_{10}O_{14}(OH)_2$ (see below). However, it was often rather light green. Moreover, when the precipitate is not treated with acid in order to preserve the aluminium hydrate as an extender, the precipitate could turn completely brown, spoiling the pigment. It had already been mentioned in eighteenth- and nineteenth-century books that washing of the pigment was critical in order to obtain an intense blue color.

Five samples from successful syntheses, as well as one sample from an unsuccessful synthesis, which led to the production of a brown powder, were selected for further analyses (see Table 2). A commercial Prussian blue pigment was purchased as reference from Sigma-Aldrich.

### 2.2. Fading experiments

The five blue powders were mixed with a 10% gum arabic binder in aqueous solution in a pigment-to-binder 1:2 weight-to-weight ratio. The mixtures were painted onto 2 cm$^2$ 100% cotton watercolor paper. In watercolor painting white pigments are rarely employed because the white of the paper is usually used in transparency to lighten the color. Therefore the samples were not diluted with a white pigment but were rather painted in a light shade, by decreasing the pigment concentration. The watercolor paper, the 10% gum arabic containing aqueous solution, which is manufactured by Winsor and Newton, London, England, and the brushes used for painting were purchased from the artist's material supplier Schleiper, Liège, Belgium.

The samples were subjected to accelerated light exposure fading over a period of 400 h by using a SUNTEST CPS+ weathering chamber equipped with a xenon lamp; a window glass filter that removed UV radiation below 320 nm was used to simulate indoor ageing, as is recommended in the ISO 787-15 standard. A ventilation system was used to cool the ageing chamber to a constant black standard temperature of ∼308 K. The luminance at the surface of the sample was ∼90000 lux. During the accelerated light exposure half of the painted paper surface area was covered with aluminium to serve as a reference after light exposure. Considering a museum light source with a luminance of 150 lux and an exposure time of 8 h a day, a light exposure time of 400 h at 90000 lux in a weathering instrument corresponds to approximately 82 years. For all the techniques described below and used for the characterization of the paint layers, no fading or visible color change has been observed in the samples after the measurements (see supporting information for details).

### 2.3. Mössbauer spectroscopy

The iron-57 Mössbauer spectra have been measured at 295 K with a constant-acceleration spectrometer which utilized a rhodium matrix cobalt-57 source. The Mössbauer spectral absorbers were prepared with 10 to 15 mg cm$^{-2}$ of powdered Prussian blue mixed with boron nitride, which is transparent to $\gamma$-ray radiation. The typical spectral acquisition time was one day. The spectrometer was calibrated at 295 K with $\alpha$-iron powder. The errors quoted for the Mössbauer spectral parameters are the statistical errors. More realistic errors are probably twice the statistical errors.

### 2.4. Particle-induced X-ray emission spectroscopy

The particle-induced X-ray emission measurements were carried out by using an external proton beam of ∼3.12 MeV, produced by the cyclotron of the University of Liège. Description and recent improvements of the PIXE line and extraction nozzle have been described by Weber *et al.* (2005) and Dupuis *et al.* (2010).

The emitted X-rays were detected by a lithium drifted silicon Si(Li) Sirius detector equipped with a 1 μm carbon foil and characterized by a lower quantification limit in energy of ∼1 keV. A system of helium injection is placed between the proton beam spot and the detector in order to avoid the energy loss of the incident particles as well as their energetic and spatial dispersion, and to reduce the absorption in air of low-energy *K* X-rays.

The external proton beam is collimated with a 0.5 mm-diameter collimator, resulting in a ∼1 mm-diameter spot at the sample. Because the X-ray yield is extremely high, a low-intensity proton beam of 5 nA was sufficient for this work.

The particle-induced X-ray emission spectra were analyzed using the *GUPIXWIN* software (Weatherstone *et al.*, 2000). Calibration in energy and adjustment of the experimental parameters were achieved by fitting a diorite, DR-N, standard. Prussian blue powders were analyzed in the form of pressed pellets and were considered as thick targets. The elemental composition was calculated by taking into account the invisible elements, *i.e.* the light elements that are known to be present in the sample but whose X-rays are not detected, such as the H, C, N and O; the water was not considered in the elemental composition.

### 2.5. X-ray diffraction

The powder X-ray diffraction patterns of the samples were first obtained with a PANalytical PW-3710 diffractometer with 1.9373 Å iron $K_\alpha$ radiation.

High-energy X-ray experiments were later performed in order to obtain the pair distribution function, which is best obtained by using high-energy synchrotron radiation, because the scattering signal at high $Q$ is more easily extracted. The pair distribution experiment was carried out at beamline ID11 at the European Synchrotron Research Facility, in Grenoble, France. This beamline offers a high flux over the 29 to 140 keV energy range. It is equipped with a Si(111) double-crystal monochromator and an X-ray transfocator. The beam size was $\sim$50 μm × 200 μm in area. A few milligrams of each Prussian blue sample were placed in 0.3 mm-diameter quartz capillaries in front of the detector. The X-ray energy was 99.428 keV, with a wavelength of 0.124968 Å. A total of 81 two-dimensional diffraction images per sample, with an acquisition time of 20 s per image, were collected with the ESRF FreLoN camera placed at $\sim$107 mm from the sample. These diffraction images were then averaged and integrated into a linear scattering signal with the software *fit2D* (Hammersley *et al.*, 1996). The distance between the sample and the detector was determined using a $LaB_6$ standard.

According to the formalism developed by Proffen & Billinge (1999), the pair distribution function, $G(r)$, is obtained by a Fourier transform of the total X-ray or neutron diffraction scattering pattern,

$$G(r) = 4\pi r\left[\rho(r) - \rho_0\right] = (2/\pi) \int_0^\infty Q[S(Q) - 1] \sin Qr \, \mathrm{d}Q, \quad (1)$$

where $\rho(r)$ is the microscopic pair density, $\rho_0$ is the atomic number density, *i.e.* the number of electrons per $Å^3$, $S(Q)$ is the total structure function, *i.e.* the normalized scattering intensity, and $Q$ is the magnitude of the scattering vector. For elastic scattering, $Q = 4\pi \sin\theta/\lambda$, where $2\theta$ is the scattering angle and $\lambda$ is the wavelength of the radiation. The function $G(r)$ in (1) is referred to as the reduced pair distribution function and gives the probability of finding an atom or ion at a distance $r$ from a given atom or ion. This function $G(r)$ may be extracted from X-ray diffraction data and fitted.

The pair distribution function was extracted using the *PDFgetX2* software (Qiu *et al.*, 2004). The pair distribution function was obtained by using a Gaussian damping of 10 to 20 Å$^{-1}$, and a maximum $Q$-value, $Q_{max}$, of 27 Å$^{-1}$. Finally the pair distribution function was fitted with the *PDFGui* software (Farrow *et al.*, 2007), up to 12 Å. Details of the fitting procedure are given in the supplementary material.

### 2.6. Iron *K*-edge X-ray absorption spectroscopy

The iron *K*-edge X-ray absorption near-edge experiments were performed at the DUBBLE Dutch–Belgian beamline BM26, which is located at a bending-magnet port of the European Synchrotron Radiation Facility electron storage ring; the magnet has a magnetic field induction of 0.4 T. This beamline (Nikitenko *et al.*, 2008), which is equipped with a Si(111) double-crystal monochromator, delivers an X-ray beam with an energy of 9.6 keV and a relative energy resolution, $\Delta E/E$, of $\sim$2 × $10^{-4}$. The higher harmonics were suppressed with a silicon-reflecting strip on a mirror behind the monochromator.

The energy scale was calibrated with a 4 μm-thick iron foil, whose spectrum was recorded in transmission mode and the energy of the first maximum in the derivative of the absorption at the iron *K*-edge was taken to be 7112 eV. In transmission mode the intensities of the incident and transmitted X-ray beams were measured using Oxford Instruments ionization detectors. Powders of both the eighteenth-century laboratory-synthesized and commercial Prussian blue samples have been measured in transmission mode. After appropriate mixing and grinding with boron nitride, the powders were pressed into self-supporting pellets in stainless steel sample holders.

The X-ray absorption near-edge spectral data reduction and analysis were performed with the *XDAP* software (Vaarkamp *et al.*, 1995). A modified Victoreen curve (Vaarkamp *et al.*, 1994) was used for the pre-edge background subtraction in the X-ray absorption spectra obtained in transmission mode and a linear function or a constant was used for the same subtraction in the spectra obtained in fluorescence detection mode. A cubic-spline routine was used for the atomic background subtraction (Cook & Sayers, 1981). The pre-edge background-subtracted spectra were normalized to the edge height, which was taken to be the value of the atomic background at 50 eV above the *K*-edge.

### 2.7. Raman spectroscopy

The Prussian blue powders were studied by using two spectrometers, first a Horiba Jobin Yvon LabRAM 300 Raman spectrometer equipped with a 514 nm laser with a power of 0.3 mW. All spectra are the result of the sum of two scans with an integration time of 100 s between 2800 and 100 cm$^{-1}$; the resolution is 5 cm$^{-1}$. The second spectrometer was a Renishaw inVia multiple laser dispersive Raman spectrometer equipped with a Peltier-cooled near-infrared-enhanced deep-depletion charge-coupled detector with 576 × 384 pixels and a direct-coupled Leica DMLM microscope. A 785 nm laser made by Toptica Photonics XTRA, Graefelfing, Munich, Germany, was used. Neutral density filters were used to reduce the laser power at the sample. The instrument was

calibrated by using a silicon peak. The baseline of the Raman spectra was corrected with a polynomial function.

### 2.8. UV–visible spectroscopy

For UV–visible reflectance spectroscopy, two types of instruments were employed, first a BYK-Gardner color guide and second a StellarNet EPP2000C UV–visible reflectance spectrometer. The BYK-Gardner color guide has a 45° geometry and a 4 mm aperture. A visible spectrum was recorded between 400 and 700 nm with a resolution of 20 nm, and automatically converted to the Commission Internationale de l'Eclairage 1976 unitless $L^*$, $a^*$ and $b^*$ parameters by using the standard illuminant D65 as a reference. These parameters correspond to the lightness, red–greenness and yellow–blueness, respectively, of the color and are derived from the XYZ tristimulus values of a reference white object and the colored object (Wyszecki & Stiles, 2000). In order to evaluate the degree of fading of a sample, the color difference, $\Delta E^*$, between the unexposed and the light-exposed portion of the sample was calculated from $\Delta E^* = [(\Delta L^*)^2 + (\Delta a^*)^2 + (\Delta b^*)^2]^{1/2}$. Typically, a $\Delta E^*$ color difference of less than 1 is imperceptible to the human eye.

The second UV–visible reflectance spectrometer was a StellarNet EPP2000C spectrometer equipped with a CCD detector. The optical-fiber probe consists of six illuminating fibers and a single fiber that collects the reflected light. The sample is illuminated over a surface area of approximately 4 mm$^2$ at an angle of 45° in order to avoid direct reflection; a Halon D50 white reference was used for calibration. The spectra were recorded in reflection mode between 350 and 880 nm, with a resolution of 1 nm. The absorbance spectra were then calculated using the *SpectraWiz* software.

## 3. Characterization of eighteenth-century Prussian blue pigments

### 3.1. Color

The color of each Prussian blue powder, which was mixed with gum arabic and painted on watercolor paper, was evaluated by UV–visible reflectance spectroscopy (see Fig. 1). The
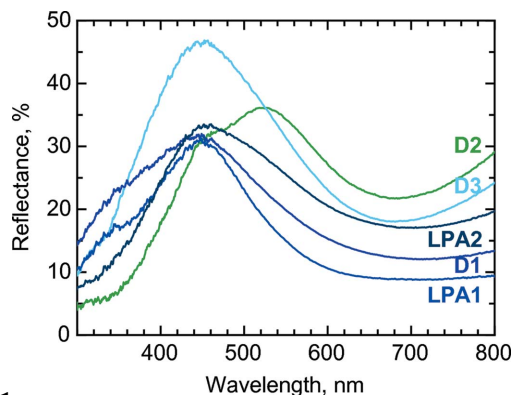


**Figure 1**
UV–visible spectra of Prussian blues prepared according to the eighteenth-century recipes, mixed with gum arabic, and painted on watercolor paper.

final pigments obtained were of variable color quality after treatment with hydrochloric acid, a color that ranged from intense blue for D1 and LPA1 to blue–gray for LPA2. The D2 and D3 samples were not treated with hydrochloric acid and hence contain a white aluminium compound as an extender; consequently they exhibit a higher reflectance because of their paler shade. This aluminium compound is usually considered as an aluminium hydroxide (Kirby & Saunders, 2004; Asai, 2005) but will be shown herein to be an alumina hydrate, $Al_{10}O_{14}(OH)_2$. D2 has a greenish tint, and its reflectance spectrum extends from a shoulder at 450 nm to a maximum at 514 nm (see Fig. 1). LPA3 was not treated with hydrochloric acid and also contained an aluminium compound but, in contrast to D2 and D3 which are light blue, LPA3 is completely brown; the UV–visible reflectance spectrum of LPA3 is not shown in Fig. 1.

### 3.2. Mössbauer spectral results

Iron-57 Mössbauer spectroscopy is the technique of choice for identifying a ferric ferrocyanide complex, such as Prussian blue, as well as for determining the possible presence of other iron-containing compounds. Moreover, Mössbauer spectroscopy, which does not require a complex sample preparation, provides bulk information on the nature of the sample, information that is relatively easy to interpret on the basis of an extensive library of previous published spectra.

The Mössbauer spectra obtained at 295 K of the laboratory-synthesized eighteenth-century samples are shown in Fig. 2. The spectra of D1 and LPA1 were fit with a model very similar to that used for modern Prussian blues (Samain *et al.*, 2011, 2012; Reguera *et al.*, 1992; Maer *et al.*, 1968; Grandjean *et al.*,
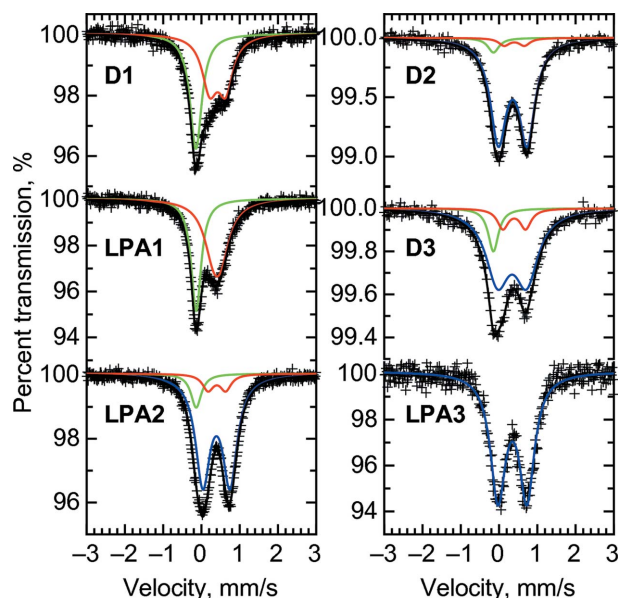


**Figure 2**
The 295 K Mössbauer spectra of eighteenth-century Prussian blue samples. The solid green and red lines represent the iron(II) and iron(III) doublets of Prussian blue, respectively. In four of the six spectra shown, ferrihydrite dominates, as is shown by the solid blue line, which corresponds to a ferrihydrite quadrupole doublet.

**Table 3**
Mössbauer spectral parameters of eighteenth-century Prussian blue samples.

| Synthesis | Assignment | $\delta$ (mm s$^{-1}$)† | $\Delta E_Q$ (mm s$^{-1}$) | $\Gamma$ (mm s$^{-1}$)‡ | $A^{II}$ (%) |
|---|---|---|---|---|---|
| D1: Dossie, immediate filtration, acid treatment | Fe(II) | −0.145 (3) | 0.06 (3) | 0.36 (2) | 47 (1)§ |
| | Fe(III) | 0.424 (8) | 0.414 (9) | 0.48 (2) | 53 (1) |
| LPA1: Le Pileur, immediate filtration, acid treatment | Fe(II) | −0.141 (2) | 0.100 (8) | 0.27 (1) | 39 (1)§ |
| | Fe(III) | 0.400 (5) | 0.18 (2) | 0.61 (2) | 61 (1) |
| D2: Dossie, no acid treatment, + alumina hydrate | Fe(II) | −0.145¶ | 0.06¶ | 0.36¶ | 5 (1)†† |
| | Fe(III) | 0.424¶ | 0.414¶ | 0.48¶ | 5 (1)†† |
| | Fh | 0.360 (5) | 0.751 (6) | 0.49 (1) | 90 (1) |
| D3: Dossie, no acid treatment, + alumina hydrate | Fe(II) | −0.145¶ | 0.06¶ | 0.36¶ | 13 (1)†† |
| | Fe(III) | 0.424¶ | 0.414¶ | 0.48¶ | 13 (1)†† |
| | Fh | 0.354 (6) | 0.785 (8) | 0.64 (1) | 74 (3) |
| LPA2: Le Pileur, delayed filtration, acid treatment | Fe(II) | −0.141¶ | 0.100¶ | 0.27¶ | 9.2 (5)†† |
| | Fe(III) | 0.400¶ | 0.18¶ | 0.350¶ | 9.2 (5)†† |
| | Fh | 0.392 (2) | 0.699 (4) | 0.433 (5) | 81 (1) |
| LPA3: Le Pileur, no acid treatment, + alumina hydrate, brown | Fh | 0.352 (3) | 0.76 (1) | 0.48 (1) | 100 |

† The isomer shift, $\delta$, is referred to $\alpha$-iron at 295 K.   ‡ $\Gamma$ is the full line width at half-maximum.   § $A^{III} = 100 - A^{II}$.   ¶ Parameter constrained to the given value.   †† $A^{III} = A^{II}$ and $100 = A^{Fh} + A^{III} + A^{II}$.

2012), *i.e.* with two Lorentzian doublets assigned to low-spin iron(II) and high-spin iron(III) (see Table 2). In contrast, samples LPA2 and the samples containing an extender, LPA3, D2 and D3, exhibit rather different Mössbauer spectra.

The Mössbauer spectrum of the brown powder, LPA3, closely resembles that of ferrihydrite (Fh). Ferrihydrite is a poorly ordered hydrous iron(III) oxide, composed of spherical particles of 2 to 7 nm diameter (Murad & Johnston, 1987). However, because of the nanocrystalline nature of ferrihydrite, the determination of an accurate stoichiometry and structure is difficult and is still an open question (Michel *et al.*, 2007). The iron-57 Mössbauer spectrum of ferrihydrite consists of a doublet with an isomer shift of $\sim 0.35$ mm s$^{-1}$ and an average quadrupole splitting of 0.70 mm s$^{-1}$ (Murad & Johnston, 1987; Mikutta *et al.*, 2008). The value of the quadrupole splitting is correlated with the crystallinity of the ferrihydrite; the poorer the crystallinity, the larger is the quadrupole splitting, a splitting that may reach 0.8 mm s$^{-1}$. Ferrihydrite is formed by the rapid oxidation of iron-containing solutions (Murad & Johnston, 1987). The production of ferrihydrite during the eighteenth-century synthesis of Prussian blue is quite likely. LPA2, D2 and D3, which exhibit only a pale blue shade, are thus believed to contain ferrihydrite as well as a small amount of Prussian blue.

The Mössbauer spectra of LPA2, D2 and D3 were fit with three components, the iron(II) and iron(III) doublets characteristic of Prussian blue and a third doublet with the spectral parameters of ferrihydrite. The spectral parameters, except the relative area, for both Prussian blue doublets were constrained to the values obtained in D1 and LPA1 for D2 and D3 and LPA2, respectively. The percent areas of both Prussian blue doublets were constrained to be equal, *i.e.* $A^{II} = A^{III}$. The ferrihydrite isomer shift, $\delta^{Fh}$, and quadrupole splitting, $\Delta E_Q^{Fh}$, the full line width at half-maximum of ferrihydrite, $\Gamma^{Fh}$, and the iron(II) percent area, $A^{II}$, were adjusted; the resulting Mössbauer spectral parameters are given in Table 3.

Among the iron ions in LPA2 and D3, only $\sim 20$ to 25% are found to be a part of Prussian blue. For D2 this fraction decreases to 10%. The large amount of ferrihydrite, which is

red–orange in color, as are other iron oxides, could explain the color shift from blue to blue–gray for LPA2, and from blue to light green, for D2. D3 contains somewhat more Prussian blue than D2, and appears bluer (see Fig. 1). Particles of ferrihydrite can be easily identified in optical micrographs (see



*(a)*



*(b)*
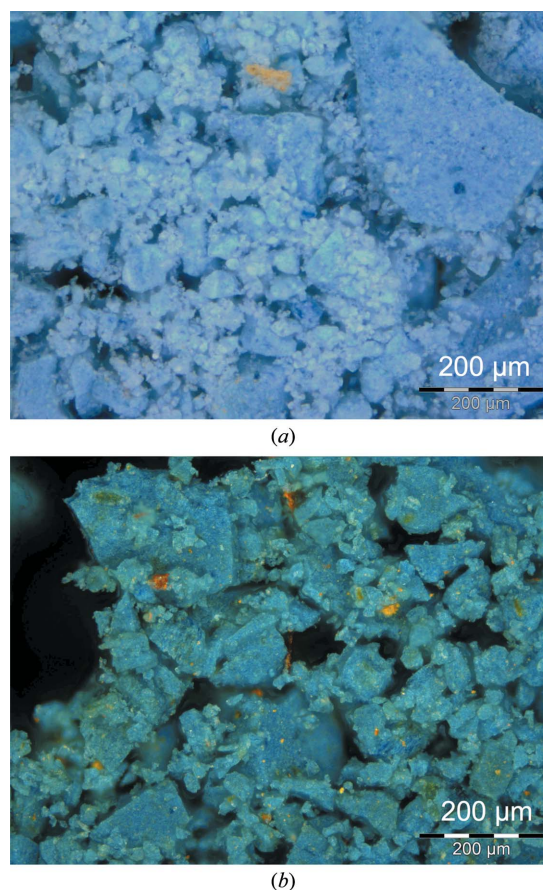
**Figure 3**
Optical micrographs of eighteenth-century Prussian blues that were not treated with hydrochloric acid and that contain alumina hydrate: (*a*) D3 and (*b*) D2. The micrographs have been obtained with reflected visible light and dark-field illumination. The orange particles contain ferrihydrite.

**Table 4**
Particle-induced X-ray emission analyses of eighteenth-century Prussian blue pigments.

| Sample | Element (wt%)† | | | | | | | | |
|---|---|---|---|---|---|---|---|---|---|
| | Na | Al | Si | P | S | Cl | K | Ca | Fe |
| D1‡ | – | – | 0.4 (1) | 0.2 (1) | 0.7 (1) | 0.5 (1) | 0.7 (1) | 0.1 (1) | 40.0 (3) |
| D2§¶ | – | 24.0 (3) | – | 1.3 (1) | 8.5 (2) | – | 0.2 (1) | – | 13.5 (2) |
| D3§¶ | – | 28.9 (5) | 0.3 (1) | 1.0 (1) | 8.0 (2) | – | 0.1 (1) | – | 19.6 (7) |
| LPA1‡ | – | 0.2 (1) | 0.2 (1) | 1.1 (1) | 0.9 (1) | 0.1 (1) | 7.4 (1) | – | 37.2 (2) |
| LPA2§ | – | 3.6 (2) | 0.6 (1) | 14.6 (2) | 1.5 (1) | – | 0.7 (1) | – | 49.2 (4) |
| LPA3§¶ | 0.3 (1) | 12.7 (2) | 0.5 (1) | 0.6 (1) | 2.0 (1) | – | 0.7 (1) | – | 30.7 (2) |
| Blood†† | 7.4 (7) | 3.4 (4) | – | 7.8 (3) | 12.8 (4) | 13.8 (4) | 29.7 (6) | 16.2 (6) | 3.1 (3) |

† The values given in parentheses are the statistical errors and the fit error given by *GUPIXWIN*. The concentration is calculated by taking into account the undetectable elements, H, C, N and O, as stoichiometrically tied to iron or aluminium cations in the following ratios: ‡ Fe:C:N ratio of 1:3:3. § Fe:O:H ratio of 1:2:1. ¶ Al:O:H of 1:3:3. †† The results for the dried blood used in the preparations.

Fig. 3). In addition to Prussian blue and ferrihydrite, both D2 and D3 contain a large amount of a white aluminium compound, shown herein to be alumina hydrate, $Al_{10}O_{14}(OH)_2$ (see below). The dominant blue in these three powders highlights the very high tinting strength of Prussian blue, which very efficiently colors the alumina hydrate. The relatively large ferrihydrite quadrupole splitting of 0.71 to 0.76 mm s$^{-1}$ suggests a poor crystallinity of ferrihydrite in the powders.

Prussian blue can also be identified by using a vibrational spectral technique, such as Raman spectroscopy, because of its sharp CN$^-$ stretching bands, $\nu$(CN), in the 2000 to 2200 cm$^{-1}$ region of the spectrum. The Raman spectra of the laboratory-synthesized powders LPA1, LAP2 and D3 exhibit the two characteristic strong $\nu$(CN) bands at $\sim$2150 and 2088 cm$^{-1}$, bands that confirm the presence of Prussian blue (see Fig. 4). The shoulder at 2120 cm$^{-1}$ may indicate the presence of a co-precipitated ferricyanide ion (Xia & McCreery, 1999). Lower-frequency Raman bands arise from iron–ligand vibrations, such as $\nu$(Fe—C), $\delta$(Fe—CN) and $\delta$(C—Fe—C) (Nakamoto, 1978; Barsan *et al.*, 2011). In contrast with LPA1, which exhibits sharp bands, LPA2 and D3 exhibit broadening that is most likely caused by the presence of nanoparticles.

The very broad bands in the 600 to 1800 cm$^{-1}$ region of the Raman spectra of LPA2 and D3 can be attributed to either nanocrystalline ferrihydrite or alumina hydrate. Although LPA2 and D3 only contain about 20% of Prussian blue *versus* 80% of ferrihydrite, the signal of Prussian blue appears much stronger than those of ferrihydrite. Consequently, on the basis of the Raman spectra alone, one would be tempted to conclude that there is a substantial amount of Prussian blue, whereas there is actually a much larger amount of iron(III) oxide. This misinterpretation is worth noting because Raman spectroscopy is often used for pigment identification in paint layers from cultural heritage objects.

### 3.3. Elemental composition

The Prussian blue powders were analyzed by particle-induced X-ray emission measurements in order to determine their elemental composition (see Table 4). As expected, the samples that were not treated with hydrochloric acid, *i.e.* D2, D3 and LPA3, have a relatively high aluminium content. The iron content in the LPA1 and D1 pigments is in agreement with the previous analytical results obtained on modern Prussian blues (Samain *et al.*, 2012). LPA1 contains potassium cations whereas D1 does not. One should note the relatively high phosphorus and sulfur content present in all samples, as well as the small aluminium content detected in LPA1 and LPA2, which were nevertheless treated with hydrochloric acid; these contents most likely come from the dried blood used as a starting reagent.

### 3.4. Crystal structure

The X-ray powder diffraction patterns obtained with iron $K_\alpha$ radiation are shown in Fig. 5. The Prussian blue samples, LPA1 and D1, exhibit a diffraction pattern that is similar (Samain *et al.*, 2012) to that of commercial Prussian blue. However, the diffraction lines are broadened, a broadening that indicates the presence of nanoparticles and strain. Particle size and strain were estimated by the Williamson–Hall method (see the electronic supplementary material for details). LPA1 contains particles of $\sim$60 nm diameter, whereas D1 contains particles of $\sim$18 nm diameter, in the (*h*00) crystallographic direction. The strain in both samples is evaluated from the slope of the linear regression of the Williamson–Hall plot and is equal to 0.37 and 0.89% in LPA1 and D1, respectively. In agreement with the correlation
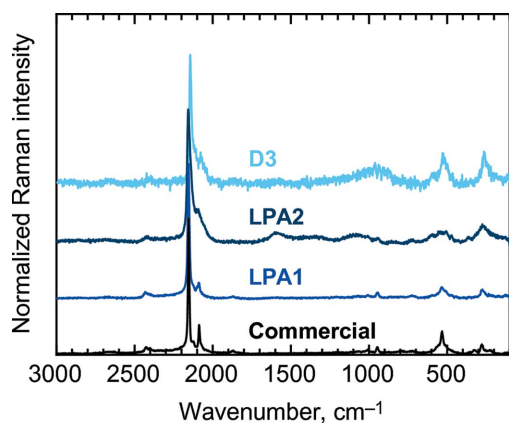


**Figure 4**
Raman spectra of eighteenth-century and commercial reference Prussian blues. All spectra are normalized according to the intensity of their most intense vibrational band. All pigments exhibit a $\nu$(CN) band at 2150 cm$^{-1}$, a band that is characteristic of ferrocyanide complexes.
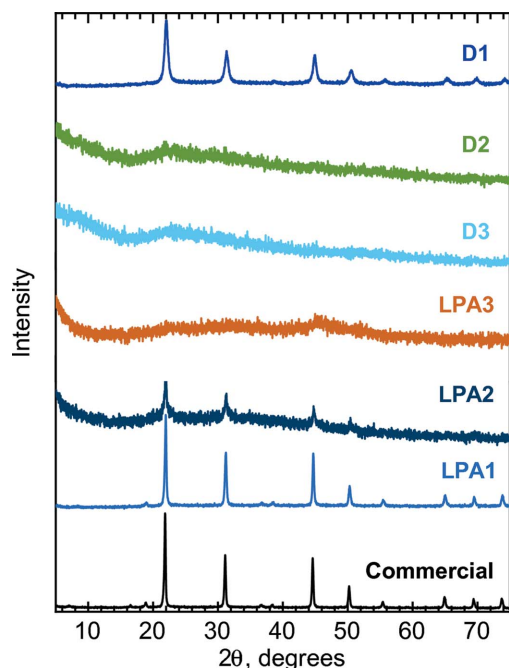
**Figure 5**
X-ray powder diffraction patterns of eighteenth-century Prussian blues.

between iron(III) quadrupole splitting and strain observed on modern Prussian blue powders (Samain *et al.*, 2012; Grandjean *et al.*, 2012), D1 exhibits an iron(III) quadrupole splitting of 0.42 (1) mm s$^{-1}$, a splitting that is characteristic of a large strain, whereas LPA1 exhibits a smaller iron(III) quadrupole splitting of 0.18 (2) mm s$^{-1}$, that is characteristic of a small strain.

LPA2, which contains a large amount of ferrihydrite, exhibits significantly broadened diffraction peaks and an intense amorphous background. All three powders that were not treated with acid, D2, D3 and the brown powder LPA3, show an amorphous diffraction pattern. X-ray powder diffraction does not provide suitable data for structural investigations of the latter samples because all the Bragg peaks are strongly broadened or non-existent because of intrinsic disorder. This disorder results in the occurrence of diffuse scattering, which contains information about two-body interactions. It can be studied by pair distribution function analysis.

### 3.5. Pair distribution function analysis

The eighteenth-century Prussian blue samples were analyzed by high-energy X-ray diffraction in order to extract the pair distribution function from the total scattering signal by Fourier transform. The pair distribution of the laboratory-synthesized eighteenth-century powders

are shown in Fig. 6. The pair distribution of the commercial Prussian blue is shown as a reference.

The pair distributions of the LPA2, LPA3 and D2 eighteenth-century Prussian blues are dramatically different from those of the modern Prussian blues (Samain *et al.*, 2012). The strong signal attenuation above 10 Å suggests nanocrystalline powders. The structure of the brown powder LPA3 can be fully described by using the model of nanocrystalline alumina hydrate, tohdite, or $Al_{10}O_{14}(OH)_2$ (see Fig. 6). The name tohdite refers to the synthetic alumina hydrate phase, whereas akdalaite is the natural form of alumina hydrate (Yamaguchi *et al.*, 1963). Both compounds were eventually shown to have the same structure and composition and are described by the hexagonal *P63mc* space group with $a$ = 5.58 (1) and $c$ = 8.86 (2) Å (Hwang *et al.*, 2006). In 2007 Michel *et al.* (2007) determined through pair distribution analysis a similar structure and composition for nanocrystalline ferrihydrite, $Fe_{10}O_{14}(OH)_2$, with lattice parameters $a \simeq 5.95$ and $c \simeq 9.06$ Å. Ferrihydrite, $Fe_{10}O_{14}(OH)_2$, and alumina hydrate, $Al_{10}O_{14}(OH)_2$, exhibit a very similar pair distribution because they are isostructural.

The average crystallite size in LPA3 is 15 Å and the unit-cell parameters are $a$ = 5.96 (2) and $c$ = 8.64 (3) Å. On the basis of the Mössbauer spectral and particle-induced X-ray emission analyses, one can conclude that LPA3 contains nanocrystalline alumina hydrate as well as nanocrystalline ferrihydrite. The brown hue of LPA3 is an additional indication of the presence of an orange iron oxide, as white alumina hydrate would not color the powder.

As is indicated by the particle-induced X-ray emission and Mössbauer analysis, D2 is expected to contain a large amount of alumina hydrate, ferrihydrite and a small amount of Prussian blue. On the basis of the structural composition of LPA3, the pair distribution of D2 was refined by using the structural
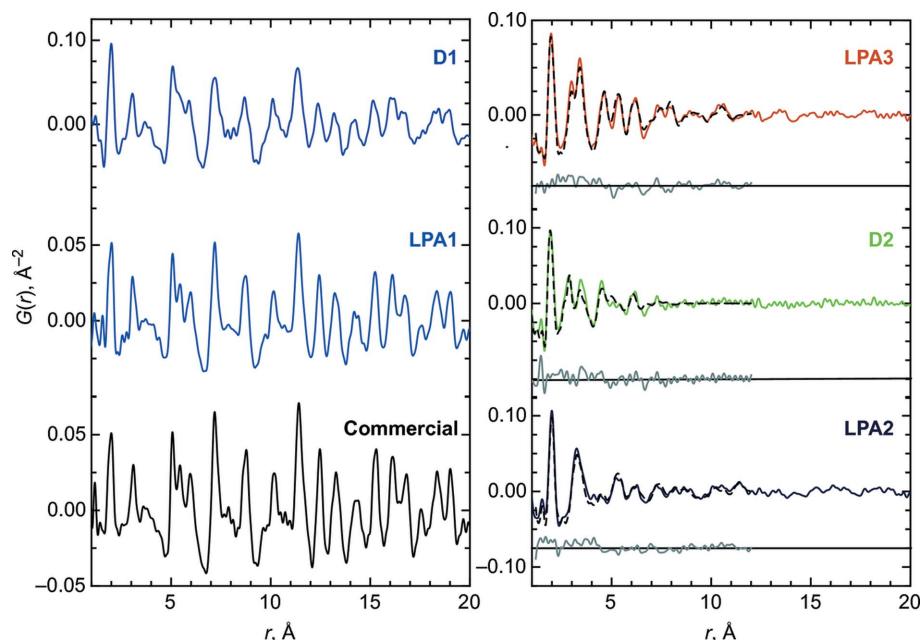


**Figure 6**
The pair distribution function for the eighteenth-century and commercial Prussian blue pigments. Experimental data and fit are shown by the colored solid and black dotted line, respectively.

phase of nanocrystalline alumina hydrate (see Fig. 6). Attempts to fit the pair distribution with additional phases in order to take into account the presence of ferrihydrite and Prussian blue in D2 result either in negative relative phase contents or unlikely lattice parameters. The discrepancy between the observed data and the calculated pair distribution can be attributed to the particularly large amount of impurity in D2, *i.e.* phosphorus and sulfur contents of 1.3 and 8.5 wt%, respectively.

The LPA2, LPA3 and D2 samples were treated with hydrochloric acid in order to eliminate the extender, *i.e.* alumina hydrate. According to the Mössbauer spectral results, LPA2 is mainly composed of ferrihydrite, whereas D1 and LPA1 are rather pure Prussian blues. Indeed, the pair distributions of D1 and LPA1 are very similar to that of commercial Prussian blue. Fitting the pair distribution of Prussian blue is a complex task because of its inherent disorder and vacancy distribution. The method for fitting the pair distribution function by taking into account the distribution of vacancies inside the lattice is described elsewhere (Samain *et al.*, 2012; Samain, 2012) and is not reported herein.

The pair distribution of LPA2 was fit by combining the structural models of ferrihydrite and Prussian blue. Because of the restricted data range and in order to avoid overfitting the pair distribution, the structural model for Prussian blue was restricted to the most probable ordered structure, *i.e.* a structure containing one vacancy (Herren *et al.*, 1980) (see the supplementary material for details). The pair distribution refinement parameters for LPA2 revealed a relative phase content in terms of mass of 87 (1) and 13 (1)% for ferrihydrite and Prussian blue, respectively. According to the molecular mass of both compounds, 92 (1)% of the iron ions in LPA2 are part of the ferrihydrite whereas only 8 (1)% is part of the Prussian blue. In comparison with the Mössbauer spectral results, the Prussian blue content is underestimated. Nevertheless both techniques revealed the same tendency, *i.e.* the large dominance of the ferrihydrite phase in comparison with the Prussian blue phase.

The refined parameters for LPA1, D2 and D3 are available in Tables S1 and S2 in the electronic supplementary material. The agreement between the observed and the calculated pair distributions for LPA2, LPA3 and D2 is not perfect. Because of the empirical character of the recipes for their preparation, these samples contain a relatively large amount of impurities, as is shown by the particle-induced X-ray emission analysis. These impurities are probably localized in the lattice cavities of the pigment but they were not taken into account in the structural model.

### 3.6. Iron *K*-edge X-ray absorption spectroscopy

The eighteenth-century Prussian blues were finally analyzed by iron *K*-edge X-ray absorption spectroscopy. The X-ray absorption near-edge spectra are shown in Fig. 7. The spectra of LPA1 and D1 strongly resemble the typical spectrum of Prussian blue. In contrast, the spectra of the samples containing ferrihydrite, as shown by Mössbauer spectroscopy,
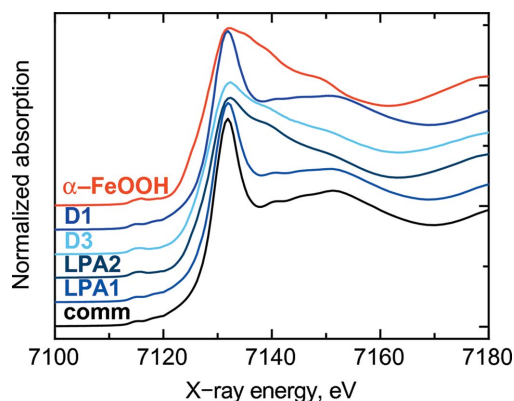


**Figure 7**
The iron *K*-edge X-ray absorption near-edge spectra of eighteenth-century Prussian blues, a commercial Prussian blue (comm) and goethite, $\alpha$-FeOOH.

are close to that of goethite, $\alpha$-FeOOH, which is the most common of the ferric oxyhydroxides. Like ferrihydrite, the goethite structure can be considered as a hexagonal close-packed array of oxygen and hydroxyl ions with the iron(III) ions occupying octahedral positions. In goethite, these octahedral positions are arranged in double rows along [001]. In ferrihydrite, some of the iron octahedral positions are vacant (Murad & Johnston, 1987). According to Wilke *et al.* (2001) the iron *K*-edge X-ray absorption near-edge spectra of goethite and ferrihydrite are very similar.

## 4. Discussion of eighteenth-century preparations

The Le Pileur d'Apligny and Dossie recipes lead to the formation of a Prussian blue pigment that at times may be of similar quality to that of modern commercial pigments, as is the case for samples LPA1 and D1. However, these recipes may at times result in the production of blue-colored pigments that cannot be considered to be Prussian blues, as is the case for the blue–gray LPA2 sample, which consists mainly of nanocrystalline ferrihydrite. Similarly, the D2 and D3 samples, although pale blue because they were not treated with hydrochloric acid, are not Prussian blue pigments but rather are largely composed of poorly ordered hydrous iron oxide or ferrihydrite, $Fe_{10}O_{14}(OH)_2$, and of alumina hydrate, $Al_{10}O_{14}(OH)_2$.

The formation of the undesirable hydrous iron oxide, identified as nanocrystalline ferrihydrite, occurs during the synthesis and, most likely, before the filtration of the pale blue–green precipitate, a precipitate that results from the reaction between the potassium hexacyanoferrate and iron(II) sulfate. The reaction immediately yields ferrous ferrocyanide, also known as Berlin white or Everitt's salt, $[Fe^{II}Fe^{II}(CN)_6]^{2-}$, through the reaction,

$$Fe^{II}(aq) + \left[Fe^{II}(CN)_6\right]^{4-}(aq) \rightarrow \left[Fe^{II}Fe^{II}(CN)_6\right]^{2-}(s).$$
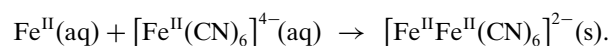
The resulting ferrous ferrocyanide is rapidly oxidized in air to yield Prussian blue. The precipitate retains a pale color because of the presence of a large amount of a white alumi-

nium compound that has been identified as alumina hydrate, $Al_{10}O_{14}(OH)_2$, by pair distribution function analysis and is formed by the hydrolysis of the aluminium(III) cation arising from alum, $KAl(SO_4)_2.12 H_2O$, which is used as one of the starting reagents.

According to the above chemical reaction, the formation of ferrous ferrocyanide requires a stoichiometric amount of iron(II) and $[Fe^{II}(CN)_6]^{4-}$. The iron(II) ions are provided by the iron(II) sulfate solution, used as a starting reagent, whereas the $[Fe^{II}(CN)_6]^{4-}$ ions are derived from the blood calcination with potassium carbonate; the hexacyanoferrate(II) anion is most likely the limiting reagent. Consequently, iron(II) ions from iron(II) sulfate remain in excess in the aqueous solution after precipitation of ferrous ferrocyanide. However, iron(II) ions are easily oxidized to iron(III) ions; the latter can then hydrolyze to produce an iron oxide, such as ferrihydrite, which is known to be formed by rapid oxidation of iron-containing solutions. Rapid filtration immediately following the precipitation prevents the formation of the orange hydrous iron oxide on the surface of the blue–green precipitate and, thus, preserves the color and nature of Prussian blue as was the case for LPA1 and D1.

The particle-induced X-ray emission measurements revealed a non-negligible amount of phosphorus in some eighteenth-century Prussian blue samples, especially in LPA2. The possibility that phosphorus may be associated with iron(III) in an iron(III) phosphate has been considered. At 295 K, iron(III) phosphate is characterized (Piña *et al.*, 2010) by a doublet with an isomer shift of 0.31 to 0.35 mm s$^{-1}$ and a quadrupole splitting of 0.6 to 0.75 mm s$^{-1}$. These parameters are very similar to those of ferrihydrite. Hence, it is virtually impossible to distinguish iron(III) phosphate from ferrihydrite on the basis of their hyperfine parameters and in the presence of the observed broad lines in the Mössbauer spectra. The presence of any iron(II) phosphate can be excluded because no characteristic absorption at 2.5 mm s$^{-1}$ is observed. In contrast, the presence of a large amount of iron(III) phosphate can be excluded on the basis of the XANES results, because the XANES spectrum of $FePO_4$ is very different from that of ferrihydrite (Wilke *et al.*, 2001). In conclusion, the main impurity iron phase in the eighteenth-century pigments is ferrihydrite, as indicated by X-ray diffraction and X-ray absorption spectroscopy results, although the presence of a small amount of iron(III) phosphate cannot be unambiguously excluded.

## 5. Color change in painted layers of eighteenth-century Prussian blue pigments

The fading under accelerated light exposure of five eighteenth-century and four modern commercial Prussian blue pigments, painted from gum arabic in dark and light blue shades, has been investigated. Fig. 8 shows the paint layers prepared on watercolor paper after the accelerated fading experiment. One half of the painted surface area, delineated by rectangles, was covered with aluminium during the expo-
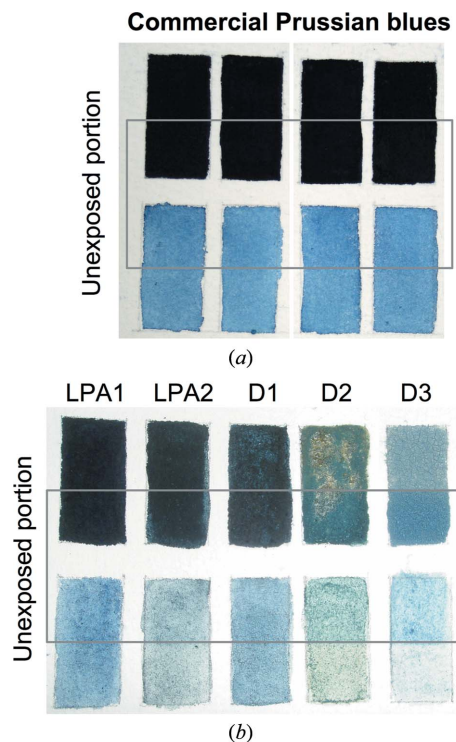


**Figure 8**
The paint layers prepared on watercolor paper. Dark and light shades (*a*) of the pure commercial Prussian blues and (*b*) of the eighteenth-century Prussian blues. The rectangles delineate the location of the aluminium cover during the accelerated light exposure.

sure and serves as a reference to appreciate the degree of fading.

Qualitatively pure commercial Prussian blue pigments painted in the dark blue shade do not exhibit any discoloration upon light exposure. In contrast, a virtually unnoticeable fading is observed for the lighter shades, *i.e.* for a lower concentration of the Prussian blue pigment; the effect of the concentration of the pigments on the degree of fading is well known (Egerton & Morgan, 1970; Sanyova, 2001).

As may be seen in Fig. 8, the paint layers containing Prussian blues synthesized according to the eighteenth-century methods exhibit a different fading behavior upon light exposure. Samples containing a fraction of ferrihydrite, such as LPA2, or alumina hydrate, such as D2 and D3, fade more strongly than LPA1 and D1.

The final color change in the four commercial and five eighteenth-century samples painted from gum arabic has been determined by colorimetric measurements. The red–greenness, $\Delta a^*$, and yellow–blueness, $\Delta b^*$, differences for these samples after 400 h of light exposure are shown in Fig. 9. The eighteenth-century samples differ significantly from the commercial samples by an increase in $\Delta b^*$, *i.e.* a loss of blue leading to a more yellow tint. The samples that exhibit the highest increase in $\Delta b^*$, *i.e.* the samples that are circled by an oval in Fig. 9, are the LPA2, D2 and D3 samples, samples that all contain a large amount of ferrihydrite that precipitated during the synthesis. These samples also show an increase in $\Delta a^*$, *i.e.* an increase in redness that can be attributed to the presence of the orange ferrihydrite that becomes more visible
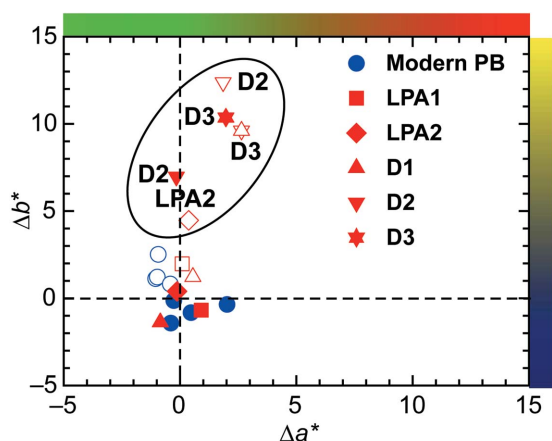
**Figure 9**
Color change observed after 400 h light exposure in commercial and eighteenth-century Prussian blue pigments painted from gum arabic in both dark and light shades. The blue points correspond to commercial Prussian blue painted in dark shade (solid points) and light shade (open points), and the red symbols correspond to eighteenth-century Prussian blues, painted in dark shade (solid symbols) and light shade (open symbols). $\Delta a^*$ corresponds to the transition from green to red, shown at the top, and $\Delta b^*$ corresponds to the transition from blue to yellow, shown at the right. The values inside the oval are for LPA2, D2 and D3, all of which contain ferrihydrite.

as the paint layer fades. The LPA1 and D1 samples, which contain only Prussian blue and no alumina hydrate or iron oxide, have a similar fading behavior as the commercial Prussian blues. The enhanced tendency of samples containing ferrihydrite to turn green was also shown by UV–visible reflectance spectroscopy as a shift in the maximum in the reflectance towards longer wavelengths (see Fig. S2 in the supplementary material).

The preparative methods clearly play a role in the fading of Prussian-blue-containing paint layers because they can lead to the production of ferrihydrite mixed with Prussian blue. This undesirable hydrous iron oxide causes the paint layer to turn green because upon ageing the Prussian blue present fades and the orange tint of the iron oxide becomes more apparent.

## 6. Analysis of a genuine paint fragment

In order to support the results obtained on laboratory-synthesized Prussian blues, a genuine paint fragment from an eighteenth-century polychrome sculpture has been analyzed.

The guardian angel shown in Fig. 10 is located in the Assumption Church of La Gleize, in the Belgian Ardennes. This large linden wood sculpture with dimensions of 133 × 110 cm dates from the beginning of the eighteenth century. However, the guardian angel of La Gleize differs in style from other seventeenth- and eighteenth-century barocco sculptures of angels. The guardian angel of La Gleize is remarkable for its polychrome character, which is unusual for the Belgian Ardennes (Cession *et al.*, 1994–1995). The polychromy was studied in 1994–1995 during the restoration of the sculpture at the Royal Institute for Cultural Heritage in Brussels (Cession *et al.*, 1994–1995). The pigment analysis revealed the presence of Prussian blue mixed with alumina hydrate in the interior of



**Figure 10**
Guardian angel, a polychrome 133 cm × 110 cm linden wood sculpture from the early eighteenth century located at the Assumption church in La Gleize, Belgium.

the angel's dress and on its sandals. The presence of Prussian blue in the original paint layers of the guardian angel provides a *terminus ante quem non* because the sculpture cannot be dated before the discovery of Prussian blue in 1704. The binder in the blue paint fragments has been identified by gas chromatography/mass spectrometry as linseed oil (Cession *et al.*, 1994–1995).

Photomicrographs of the cross section prepared from a paint fragment from the angel's right sandal are shown in Fig. 11. According to Cession *et al.* (1994–1995) four different layers can be identified, as indicated by the numbers in the optical micrograph of the cross section shown in Fig. 11(*a*). The elemental composition of each paint layer has been previously determined by scanning electron microscopy coupled with energy-dispersive X-ray spectrometry (Cession *et al.*, 1994–1995) (see Fig. S3 in the electronic supplementary material for details). The first thick white layer corresponds to a chalk ground layer and mainly contains calcium ions. The second gray layer is the proteinic isolation layer made of animal glue with a small amount of gypsum and a zinc salt, which strongly reflects UV light (see Fig. 11b). The third layer is composed of Prussian blue, alumina hydrate and lead white. A few small orange grains can be seen in this layer. Their elemental composition did not significantly differ from that of the third paint layer, with lead and aluminium ions as major elements and traces of iron and potassium ions. The upper layer is a retouching layer that was not originally present on the sculpture. It presumably contains cerulean blue, a cobalt(II) stannate, mixed with calcite and magnesia extenders.

The large dark blue particles observed in the optical photomicrographs contain both Prussian blue and alumina hydroxide as has been determined by energy-dispersive X-ray spectral mapping (see the supporting information for details). Hence, Prussian blue was synthesized according to the eight-
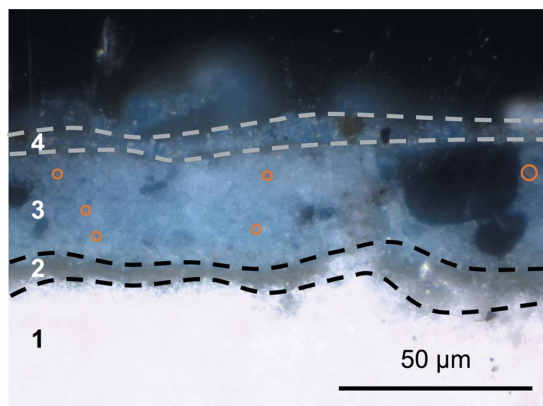
*(a)*
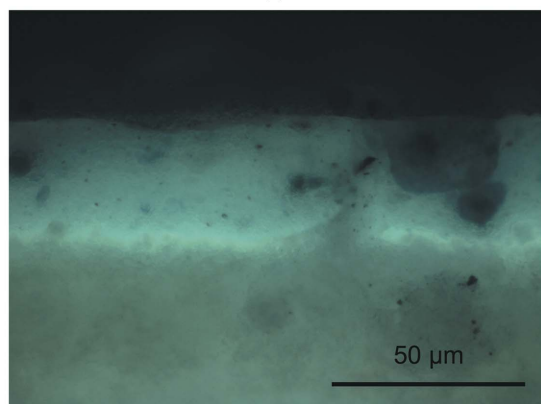


*(b)*

**Figure 11**
Optical photomicrographs of a cross section obtained with a dark-field illumination from the guardian angel of La Gleize, with (*a*) visible reflected light and (*b*) UV reflected light. The cross section consists of four different layers (see supporting information for details). Some small orange grains are indicated by orange open circles.



**Figure 12**
Raman spectra obtained on a cross section of a blue fragment from the guardian angel of La Gleize by using a 785 nm laser and a reference spectrum of raw Sienna obtained from the database of the Royal Institute for Cultural Heritage. Right: an expanded view of the $CN^-$ stretching vibration region.

eenth-century preparative method, in which alum was used as a starting reagent. After precipitation of Prussian blue, the alumina hydrate could remain as an extender to lighten the dark color of Prussian blue.

The cross section shown in Fig. 11 was analyzed by Raman spectroscopy; the resulting spectra are shown in Fig. 12. In layer 3, the spectrum obtained on the light blue area differs from that obtained on the dark blue grains because of the presence of lead white, as is indicated by the peak at $1050 \text{ cm}^{-1}$. The characteristic band for alumina hydrate could not been found in the Raman spectra. For both analysis spots the Prussian blue exhibits similar $CN^-$ stretching vibrational bands. The intermediate band at $2130 \text{ cm}^{-1}$ and the relatively large intensity of the band at $2090 \text{ cm}^{-1}$ suggest the presence of degraded Prussian blue, *i.e.* partially oxidized and reduced Prussian blue (Samain *et al.*, 2011). Although it is difficult to detect a visual fading on the basis of the cross section, the original Prussian blue paint layers on the polychrome sculpture were probably discolored.

The Raman spectrum obtained on a small orange grain suggested a molecular composition close to that of raw Sienna (see Fig. 12). Raw Sienna, a clay and an iron(III) oxyhydr-

oxides and iron(III) oxides mixture, is a yellow–brown pigment (Eastaugh *et al.*, 2008). The formation of ferrihydrite, an orange hydrous iron(III) oxide compound, was observed in eighteenth-century laboratory-synthesized Prussian blues. Thus, the presence of some orange particles of an iron(III) oxide compound most likely results from the eighteenth-century preparative method of Prussian blue. Because no silicon was detected in the orange grains by energy-dispersive X-ray spectral punctual analysis, these orange particles cannot result from the deliberate addition of any ochre, *i.e.* a mixture of clay and iron oxide, in the Prussian blue mixture. Moreover the Raman spectrum obtained on this orange grain is similar to that of iron(III) oxyhydroxide, goethite (de Faria & Lopes, 2007). The analysis of this genuine paint layer thus supports the conclusions drawn from the results obtained on laboratory-synthesized eighteenth-century Prussian blues.

The detection of both Prussian blue and an iron(III) oxide in a paint layer from a cultural heritage object indicates that the pigment used was most likely prepared according to eighteenth-century recipes of Prussian blue. This directly provides a marker for dating the art object or the paint layer between 1704, year of the invention of Prussian blue, and ~1850, *i.e.* before the introduction of modern preparative methods for Prussian blue.

## 7. Conclusions

Multiple reproductions of two different eighteenth-century preparations of Prussian blue have indicated the possible formation of an undesirable iron(III) reaction product, identified herein as ferrihydrite, $Fe_{10}O_{14}(OH)_2$. The eighteenth-century methods are based on the calcination of dried blood to produce a potassium hexacyanoferrate complex, which is the first of two essential reactants for synthesizing Prussian blue. The second reactant is an iron salt. This organic process yields

only a small amount of potassium hexacyanoferrate complex, an amount that is stoichiometrically much smaller than the amount of iron salt. If the Prussian-blue-containing precipitate is not directly filtrated, the excess iron ions remaining from the iron salt in the aqueous solution form a hydrous iron(III) oxide, which gives a greenish tint to the Prussian blue pigment. When the filtrated precipitate is not treated with hydrochloric acid, a pale blue–green powder is obtained. Such variety of Prussian blue pigments has been shown to contain only a small amount of Prussian blue and mainly ferrihydrite, $Fe_{10}O_{14}(OH)_2$, as well as alumina hydrate, $Al_{10}O_{14}(OH)_2$. Because of the broad Mössbauer spectrum of ferrihydrite and the similarity between the pair distribution functions of ferrihydrite and alumina hydrate, it is not possible to distinguish between the simultaneous presence of the two hydroxides or the presence of a mixed iron–aluminium hydroxide. The presence of alumina hydrate and orange particles of hydrous iron(III) oxides are also apparent in an eighteenth-century genuine Prussian blue sample obtained from a polychrome sculpture, the guardian angel of La Gleize.

In conclusion, the results presented herein help to better understand the numerous reports of degradation of Prussian blue found in eighteenth- and nineteenth-century books and directly relate the tendency of Prussian blue to turn green to the eighteenth-century preparative methods, that easily lead to the formation of a variable but substantial amount of an undesirable iron(III) oxide.

## References

Asai, C. (2005). *Z. Kunsttechnol. Konserv.* **18**, 261.

Barsan, M. M., Butler, I. S., Fitzpatrick, J. & Gilson, D. F. R. (2011). *J. Raman Spectrosc.* **42**, 1820–1824.

Berrie, B. H. (1997). *Artist's Pigments, A Handbook of Their History and Characteristics*, Vol. 3, edited by E. W. FitzHugh, pp. 191–217. Oxford University Press.

Buxbaum, G. & Pfaff, G. (2005). *Industrial Inorganic Pigments*, 3rd ed. Weinheim: Wiley-VCH.

Cession, C., Sanyova, J. & Van Bos, M. (1994–1995). *Bull. Inst. R. Patrim. Artist.* **26**, 163–182.

Cook, J. W. J. & Sayers, D. E. (1981). *J. Appl. Phys.* **52**, 5024–5031.

Dossie, R. (1758). *The Handmaid to the Arts.* London: Nourse.

Dupuis, T., Chêne, G., Mathis, F., Marchal, A., Philippe, M., Garnir, H.-P. & Strivay, D. (2010). *Nucl. Instrum. Methods Phys. Res. B*, **268**, 1911–1915.

Eastaugh, N., Walsh, V., Chaplin, T. & Siddal, R. (2008). *Pigment Compendium, A Dictionnary of Historical Pigments.* Oxford: Elsevier Butterworth Heinemann.

Egerton, G. S. & Morgan, A. G. (1970). *J. Soc. Dyers Colour.* **86**, 242–249.

Faria, D. de & Lopes, F. (2007). *Vib. Spectrosc.* **45**, 117–121.

Farrow, C. L., Juhas, P., Liu, J. W., Bryndin, D., Božin, E. S., Bloch, J., Proffen, T. & Billinge, S. J. (2007). *J. Phys. Condens. Matter*, **19**, 335219.

Grandjean, F., Long, G. J. & Samain, L. (2012). *Mössbauer Eff. Res. Data J.* **35**, 143–153.

Hammersley, A. P., Svensson, S. O., Hanfland, M., Fitch, A. N. & Haüsermann, D. (1996). *J. High Press. Res.* **14**, 235–248.

Herren, F., Fischer, P., Ludi, A. & Haelg, W. (1980). *Inorg. Chem.* **19**, 956–959.

Hwang, S. L., Shen, P. Y., Chu, H. T. & Yui, T. F. (2006). *Int. Geol. Rev.* **48**, 754–764.

Kirby, J. (1993). *Natl Gallery Tech. Bull.* **14**, 62–74.

Kirby, J. & Saunders, D. (2004). *Natl Gallery Tech. Bull.* **25**, 73–99.

Krafft, S. (1854). *Pour l'emploi d'une nouvelle substance propre à fabriquer le bleu de Prusse*, In *Description des machines et Procédés pour lesquels des brevets d'invention ont été pris sous le régime de la loi du 5 juillet 1844, Paris*, Vol. 17, pp. 159–160.

Le Pileur d'Apligny, M. (1779). *Traité des couleurs matérérielles et de la manière de colorer relativement aux différents arts et métiers.* Paris: Saugrain et Lamy.

Maer, K., Beasley, M. L., Collins, R. L. & Milligan, W. O. (1968). *J. Am. Chem. Soc.* **90**, 3201–3208.

Mérimée, J. (1830). *De la peinture à l'huile: ou des procédés matérériels employés dans ce genre de peinture depuis Hubert et Jean Van-Eyck jusqu'à nos Jours*, pp. 176–178. Paris: Huzard.

Michel, F. M., Ehm, L., Antao, S. M., Lee, P. L., Chupas, P. J., Liu, G., Strongin, D. R., Schoonen, M. A., Phillips, B. L. & Parise, J. B. (2007). *Science*, **316**, 1726–1729.

Mikutta, C., Mikutta, R., Bonneville, S., Wagner, F., Voegelin, A., Christl, I. & Kretzschmar, R. (2008). *Geochim. Cosmochim. Acta*, **72**, 1111–1127.

Murad, E. & Johnston, J. H. (1987). *Mössbauer Spectroscopy Applied to Inorganic Chemistry*, Vol. 2, edited by G. J. Long, pp. 507–580. New York: Plenum Press.

Nakamoto, K. (1978). *Infrared and Raman Spectra of Inorganic and Coordination Compounds.* New York: Wiley-Interscience Publication.

Nikitenko, S., Beale, A. M., van der Eerden, A. M. J., Jacques, S. D. M., Leynaud, O., O'Brien, M. G., Detollenaere, D., Kaptein, R., Weckhuysen, B. M. & Bras, W. (2008). *J. Synchrotron Rad.* **15**, 632–640.

Piña, C., Arriola, H. & Nava, N. (2010). *J. Phys. Conf. Ser.* **217**, 012037.

Proffen, T. & Billinge, S. J. L. (1999). *J. Appl. Cryst.* **32**, 572–575.

Qiu, X., Thompson, J. W. & Billinge, S. J. L. (2004). *J. Appl. Cryst.* **37**, 678.

Regnier, J. D. (1855). *Cours d'expériences chimiques sur la fixité des couleurs de la peinture à l'huile, donné au palais du louvre*, Novembre–Décembre 1853, Janvier–Février 1855. Paris: Impression de J. Claye.

Reguera, E., Fernández-Bertrán, J., Dago, A. & Díaz, C. (1992). *Hyperfine Interact.* **73**, 295–308.

Riffault, J. (1850). *Nouveau manuel complet du fabricant de couleurs et de vernis.* Paris: Roret.

Samain, L. (2012). PhD Thesis, University of Liège, Belgium.

Samain, L., Gilbert, B., Grandjean, F., Long, G. J. & Strivay, D. (2013). *J. Anal. At. Spectrom.* **28**, 524–535.

Samain, L., Grandjean, F., Long, G. J., Martinetto, P., Bordet, P. & Strivay, D. (2012). *J. Phys. Chem. C.* Submitted.

Samain, L., Silversmit, G., Sanyova, J., Vekemans, B., Salomon, H., Gilbert, B., Grandjean, F., Long, G. J., Hermann, R. P., Vincze, L. & Strivay, D. (2011). *J. Anal. At. Spectrom.* **26**, 930.

Sanyova, J. (2001). PhD Thesis, Université Libre de Bruxelles, Belgium.

Vaarkamp, M., Dring, I., Oldman, R., Stern, E. & Koningsberger, D. (1994). *Phys. Rev. B*, **50**, 7872–7883.

Vaarkamp, M., Linders, J. C. & Koningsberger, D. C. (1995). *Physica B*, **208–209**, 159–160.

Weatherstone, A., Vormwald, M., Boyd, N. & Campbell, I. (2000). *The GUPIXWIN Manual and User Guide*, Version 2.1. University of Guelph, Ontario, Canada.

Weber, G., Martinot, L., Strivay, D., Garnir, H. P. & George, P. (2005). *X-ray Spectrom.* **34**, 297–300.

Wilke, M., Farges, F., Petit, P. E., Brown, G. E. Jr & Martin, F. (2001). *Am. Mineral.* **86**, 714–730.

Wyszecki, G. & Stiles, W. S. (2000). *Color Science, Concepts and Methods, Quantitative Data and Formulae*, 2nd ed. New York: John Wiley and Sons.

Xia, L. & McCreery, R. L. (1999). *J. Electrochem. Soc.* **146**, 3696–3701.

Yamaguchi, G., Yanagida, H. & Ono, S. (1963). *Bull. Chem. Soc. Jpn*, **37**, 1555–1557.